ATMOSMJ: REVISITING GATING MECHANISM FOR AI WEATHER FORECASTING BEYOND THE YEAR SCALE

A PREPRINT

Minjong Cheon

jmj541826@gmail.com

Independent Researcher
Gangnam, Seoul, South Korea

June 12, 2025

ABSTRACT

The advent of Large Weather Models (LWMs) has marked a turning point in data-driven forecasting, with many models now outperforming traditional numerical systems in the medium range. However, achieving stable, long-range autoregressive forecasts beyond a few weeks remains a significant challenge. Prevailing state-of-the-art models that achieve year-long stability, such as SFNO and DLWP-HPX, have relied on transforming input data onto non-standard spatial domains like spherical harmonics or HEALPix meshes. This has led to the prevailing assumption that such representations are necessary to enforce physical consistency and long-term stability. This paper challenges that assumption by investigating whether comparable long-range performance can be achieved on the standard latitude-longitude grid. We introduce AtmosMJ, a deep convolutional network that operates directly on ERA5 data without any spherical remapping. The model's stability is enabled by a novel Gated Residual Fusion (GRF) mechanism, which adaptively moderates feature updates to prevent error accumulation over long recursive simulations. Our results demonstrate that AtmosMJ produces stable and physically plausible forecasts for about 500 days. In quantitative evaluations, it achieves competitive 10-day forecast accuracy against models like Pangu-Weather and GraphCast, all while requiring a remarkably low training budget of 5.7 days on a V100 GPU. Our findings suggest that efficient architectural design, rather than non-standard data representation, can be the key to unlocking stable and computationally efficient long-range weather prediction.

Keywords Convolutional Neural Network (CNN) · ERA5 Reanalysis Data · Global Weather Forecasting · Gated Residual Fusion (GRF) · InceptionNeXt

1 Introduction

The accelerating impacts of climate change have stimulated a growing interest in data-driven weather prediction models, leading to the emergence of so-called *Large Weather Models (LWMs)* Chempan and contributors [2024]. These models leverage advances in artificial intelligence to provide scalable, high-resolution alternatives to traditional numerical weather prediction systems. In particular,cular, recent models such as Huawei's Pangu-Weather Bi et al. [2023], Google's GraphCast Lam et al. [2022], NeurlGCM Kochkov et al. [2023] NVIDIA's FourCastNet Pathak et al. [2022], Alibaba's Fuxi-Weather Chen et al. [2023], Microsoft's Stormer Nguyen et al. [2023], and ArchesWeather Couairon et al. [2024a] have all demonstrated impressive performance in medium-range forecasting (up to 10 days), surpassing high-resolution forecasts of operational systems such as ECMWF's HRES model in accuracy. Moreover, Fuxi's seasonal-to-seasonal (S2S) variant has recently shown skill beyond ECMWF's S2S model, marking a significant milestone in long-range AI-based forecasting Chen et al. [2024].

Despite these advances, most AI-based weather models remain confined to the medium range. Stable autoregressive prediction over extended periods, such as year-long forecasts, remains a challenging and underexplored frontier. Only a

few recent efforts have demonstrated promising long-term results Bonev et al. [2023], Karlbauer et al. [2024]. One such model is NVIDIA's SFNO (Spherical Fourier Neural Operator), which achieved stable autoregressive forecasts for an entire year (1,460 sequential 6-hour time steps) while maintaining physically plausible dynamics. This was made possible by learning a spectral representation of global weather data via spherical harmonics, allowing the model to respect the geometry of the Earth and enhancing long-range stability.

Another study is the HEALPix-based model by Karlbauer et al. Karlbauer et al. [2024], which employs a parsimonious deep learning architecture (DLWP-HPX) on a Hierarchical Equal Area isoLatitude Pixelation (HEALPix) mesh. This model forecasts a subset of atmospheric variables at 110 km resolution and supports stable autoregressive rollout beyond one year, generating realistic seasonal evolutions. A common feature of both SFNO and DLWP-HPX is the use of ERA5 reanalysis data transformed into specialized spatial representations, such as spherical harmonics or equal-area pixelations.

However, recent studies have challenged the necessity of such strong physical priors or non-standard spatial domains. Models like ArchesWeather Couairon et al. [2024a] and Microsoft's Stormer Nguyen et al. [2023] demonstrate that with efficient architectural design and carefully tuned training objectives, competitive long-term stability can be achieved even on the standard latitude–longitude grid, without resorting to spherical remapping or spectral representations. And this further leads to a central question: *Is transforming ERA5 into non-standard spatial domains truly necessary for achieving long-term stability in AI-based forecasting?* Rather than adopting alternative grids or spectral domains, we investigate whether comparable performance can be attained by models that operate directly on the conventional latitude–longitude grid. Through this, we aim to disentangle the role of architectural design from data representation in achieving stable long-term forecasts.

Our key contributions are summarized as follows:

- Our study systematically evaluates autoregressive forecasting performance using models trained directly on the standard latitude–longitude grid, without reliance on spherical or spectral transformations.
- We demonstrate that our proposed module, Gated Residual Fusion (GRF) can provide competitive long-range stability.
- Notably, AtmosMJ matches the performance of other existing state-of-the-art (SOTA) models while requiring a remarkably low computational budget of 5.7 days on a V100 GPU. Trained and evaluated at 1.5° resolution, it also demonstrates exceptional inference efficiency by generating a 500-day forecast in approximately 21 seconds.

2 Methodology

2.1 Data Description

Following the variables listed in Table 1, we utilized the European Centre for Medium-Range Weather Forecasts (ECMWF) Reanalysis v5 (ERA5) dataset, downloaded from the WeatherBench2 repository Rasp et al. [2024]. A total of 71 daily-mean atmospheric variables, aggregated from hourly data, were used. These comprised six single-level variables and five variables sampled at 13 pressure levels, extending from near the surface up to the lower stratosphere. These include essential prognostic fields such as zonal and meridional wind components, temperature, humidity, and geopotential, which are crucial to define atmospheric dynamics. In addition, orography was included as a static topographic variable. The processed dataset was represented as tensors of shape $121 \times 241 \times 71$, corresponding to a 1.5° spatial resolution. For model training and evaluation, the data was split into training (1979–2015), validation (2016–2017), and test (2018) periods.

2.2 Architecture of AtmosMJ

Our neural network architecture is a deep convolutional model inspired by InceptionNeXt Yu et al. [2024], which itself builds upon the success of efficient convolutional architectures such as KARINA Cheon et al. [2024] and DLWP-HPX Karlbauer et al. [2024]. The input data are first processed by a stem block consisting of a depthwise separable convolution followed by layer normalization, which processes the input for multi-scale feature extraction. The main body of the network consists of four stages of InceptionNeXt blocks with Geocyclic Padding Cheon et al. [2024]. To facilitate channel-wise interaction and mitigate information loss across stages, we additionally incorporate a Gated Residual Fusion (GRF) mechanism between blocks. Since the model is designed to preserve the spatial resolution of the input throughout the entire network, no downsampling or upsampling operations are applied. Finally, a depthwise convolutional layer maps the features to the target number of output variables. The overall architecture of the InceptionNeXt and GRF is illustrated in Figure 1.

Table 1: Overview of meteorological variables used from the ERA5 dataset, including pressure-level and single-level fields.

Variable name	**Short name**	**Vertical levels (hPa)**	**Units**
Pressure-level variables			
Geopotential	Z	1000, 925, 850, 700, 600, 500, 400, 300, 250, 200, 150, 100, 50	m^2/s^2
Temperature	T	1000, 925, 850, 700, 600, 500, 400, 300, 250, 200, 150, 100, 50	K
Specific Humidity	Q	1000, 925, 850, 700, 600, 500, 400, 300, 250, 200, 150, 100, 50	kg/kg
Zonal Wind	U	1000, 925, 850, 700, 600, 500, 400, 300, 250, 200, 150, 100, 50	m/s
Meridional Wind	V	1000, 925, 850, 700, 600, 500, 400, 300, 250, 200, 150, 100, 50	m/s
Single-level variables			
2m Temperature	T2m	-	K
Mean Sea Level Pressure	MSL	-	Pa
Surface Pressure	SP	-	Pa
Total Column Water Vapor	TCWV	-	kg/m^2
Orography	OROG	-	m
TOA Incident Solar Radiation	TISR	-	J/m^2

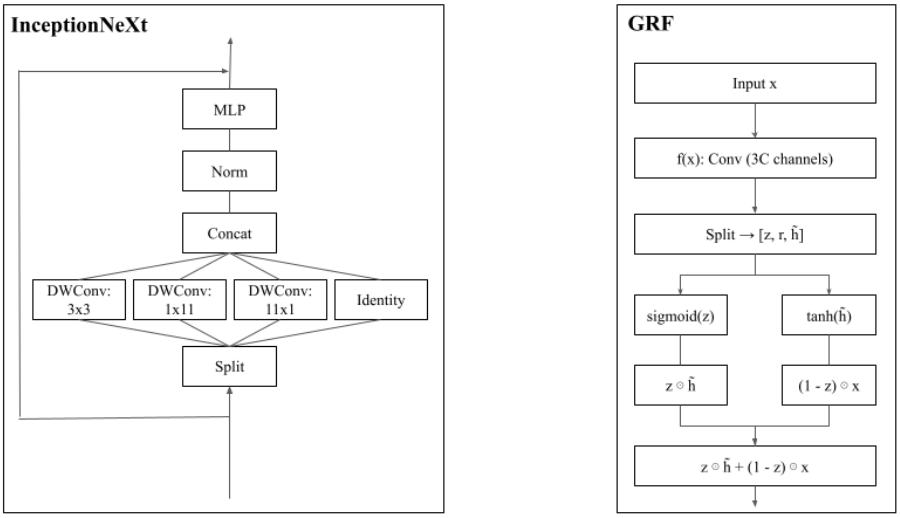

Figure 1: Main architecture of the proposed AtmosMJ model for global weather forecasting. The InceptionNeXt block (left) performs multi-scale depthwise convolution and channel mixing via MLP, while the GRF block (right) applies a gated residual fusion using update and candidate branches from a 3-way split.

2.3 Gated Residual Fusion (GRF)

Long-term autoregressive simulations require models to maintain stability over hundreds of recursive steps. To this end, we propose **Gated Residual Fusion (GRF)**, a gating mechanism designed to mitigate error accumulation by controlling the balance between the newly transformed features and the original input. The GRF module is typically applied at the end of each network block and performs the following core operation:

$$\mathbf{y} = \mathbf{z} \odot \tilde{\mathbf{h}} + (1 - \mathbf{z}) \odot \mathbf{x}, \quad \mathbf{z} = \sigma(\mathbf{z}),\ \tilde{\mathbf{h}} = \tanh(\tilde{\mathbf{h}}),$$

where $\mathbf{x}$ is the input feature, $\tilde{\mathbf{h}}$ is the candidate update, and $\mathbf{z}$ is a learnable gate that adaptively determines the contribution of each. The gating function $\sigma(\cdot)$ denotes the element-wise sigmoid activation, ensuring that the gate values remain in the range $[0, 1]$.

This soft, element-wise fusion serves multiple purposes. First, it stabilizes gradient flow: the residual branch $(1-\mathbf{z})\odot\mathbf{x}$ acts as a dynamic identity shortcut, preserving a direct path for gradients and avoiding vanishing or exploding gradients during deep updates. Second, the gate $\mathbf{z}$ selectively suppresses noise and emphasizes salient signals—when $\mathbf{z}_{i,j,k,l}\approx 0$, the output retains original information; when $\mathbf{z}_{i,j,k,l}\approx 1$, it incorporates new, non-linear structure. Third, by learning unique gates at each layer, the model can perform stage-wise routing: early stages preserve large-scale structure, while deeper stages introduce finer details. This dynamic, multi-scale control enhances both short-term accuracy and long-range consistency.

Algorithm 1: Gated Residual Fusion (GRF)

Input : Input feature tensor $\mathbf{x}\in\mathbb{R}^{B\times C\times H\times W}$
Output : Fused output $\mathbf{y}\in\mathbb{R}^{B\times C\times H\times W}$

$\mathbf{h}\leftarrow f(\mathbf{x})$; `//Pointwise Conv with` $3C$ `output channels`
$[\mathbf{z},\mathbf{r},\tilde{\mathbf{h}}]\leftarrow \text{Split}(\mathbf{h})$; `//Update, reset, candidate`
$\mathbf{z}\leftarrow\sigma(\mathbf{z})$; `//Gating with sigmoid`
$\tilde{\mathbf{h}}\leftarrow\tanh(\tilde{\mathbf{h}})$; `//Candidate transformation`
$\mathbf{y}\leftarrow\mathbf{z}\odot\tilde{\mathbf{h}}+(1-\mathbf{z})\odot\mathbf{x}$; `//Gated fusion (reset unused)`
return $\mathbf{y}$

Remark. *When $\mathbf{z}\approx 0$, the GRF behaves as an identity mapping: $\mathbf{y}\approx\mathbf{x}$. When $\mathbf{z}\approx 1$, it performs a full update: $\mathbf{y}\approx\tilde{\mathbf{h}}$. This dynamic control stabilizes long recursive rollouts by preventing feature drift and maintaining physical coherence. Unlike recurrent GRUs, GRF operates purely in a feedforward spatial context and introduces minimal computational overhead.*

2.4 Training Details

Recent AI-based weather prediction methods can be broadly categorized into three forecasting paradigms: *direct forecasting*, *continuous forecasting*, and *iterative forecasting*. In **direct forecasting**, the model is trained to predict the weather at a specific lead time T directly from the initial condition X_0, such that

$$X_T = f_\theta(X_0).$$

Continuous forecasting extends this approach by treating the lead time as an additional input, enabling a single model to predict multiple horizons:

$$X_T = f_\theta(X_0, T).$$

Iterative forecasting, on the other hand, predicts short-term increments δt and recursively feeds outputs back into the model to forecast longer sequences:

$$X_{t+\delta t} = f_\theta(X_t).$$

This iterative approach has been adopted by recent large weather models such as Stormer Nguyen et al. [2023], and GraphCast Lam et al. [2022], often with fine-tuning strategies that improve long-range stability over multiple rollout steps. Since our dataset consists of daily-resolution fields, we did not adopt roll-out based fine-tuning to avoid error accumulation and simplify the training pipeline. We utilized a weighted root mean squared error (RMSE) loss that incorporates latitude-based weighting over the global latitude–longitude grid.

$$A(\varphi_i) = N_{\text{lat}}\frac{\cos\varphi_i}{\sum_{l=1}^{N_{\text{lat}}}\cos\varphi_l} \tag{1}$$

where φ_i denotes the latitude (in radians) of the i-th grid point, and N_{lat} is the total number of latitude points. This formulation ensures that each latitude is weighted proportionally to the surface area it represents on the sphere.

where N_{lat} represents the number of grid points in the latitudinal direction.

The RMSE_l between ground truth (ERA5) $y_{t,i,j}$ and forecast $\hat{y}_{t,l,i,j}$ for lead time l is defined as follows:

$$\text{RMSE}_l = \sqrt{\frac{1}{N_{\text{time}}N_{\text{lat}}N_{\text{lon}}}\sum_{t=1}^{N_{\text{time}}}\sum_{i=1}^{N_{\text{lat}}}\sum_{j=1}^{N_{\text{lon}}}A(\varphi_i)(\hat{y}_{t,l,i,j}-y_{t,i,j})^2} \tag{2}$$

The hyperparameter setup utilized to train the AtmosMJ on the daily ERA5 dataset is described in Table 2. A time step (dt) of one day is used to train the model. A CosineAnnealingLR scheduler is used to gradually lower the learning rate during training, with the learning rate set at 0.001. The model incorporates and forecasts 71-channel inputs and outputs, which correspond to various atmospheric factors, and employs Z-score normalization. The model is trained over a maximum of 150 epochs, with AdamW serving as the optimizer for steady convergence. These parameters were selected to guarantee stable convergence and balanced learning dynamics over extended forecasts. Notably, training the model required only 5.7 days on a single V100 GPU.

Table 2: Training hyperparameters used for AtmosMJ on the ERA5 dataset.

Hyperparameter	**Value**
Loss	L2
Learning Rate (LR)	0.001
Scheduler	CosineAnnealingLR
dt	1 day
Number of In-Channels	71
Number of Out-Channels	71
Normalization	Z-score
Optimizer Type	AdamW
Max Epochs	150

3 Result

3.1 Impact of Gated Residual Fusion on Model Performance

With GRF, AtmosMJ maintains a low and stable RMSE across all three variables—even beyond 100 days of lead time—preventing the runaway error growth observed without GRF, as shown in Figure 2. In contrast, the no-GRF configuration shows a rapid, near-exponential rise in RMSE for Z500, T2m, and T850 after around day 100, with Z500 eventually exceeding 5 000 m²/s². These results highlight the effectiveness of the gated residual fusion mechanism in mitigating cumulative error growth during long-range autoregressive forecasting. Furthermore, AtmosMJ can generate a full 500-day forecast in approximately 21 seconds on a single GPU, demonstrating that GRF enables not only stability but also practical efficiency.

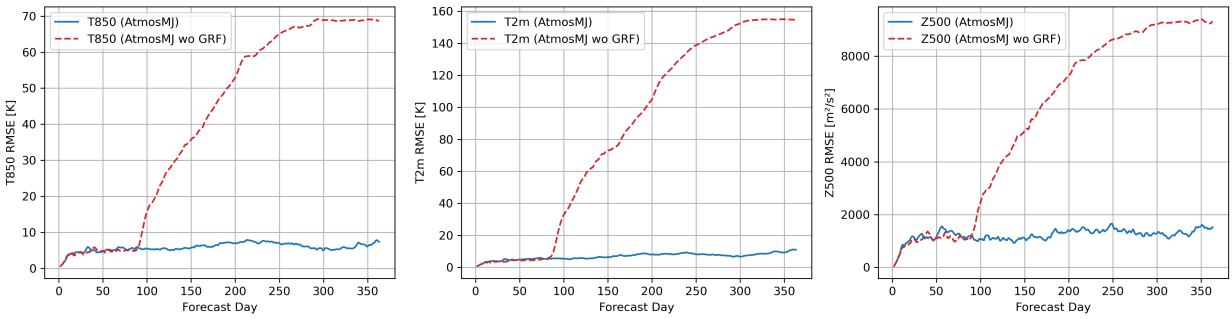

Figure 2: Latitude-weighted RMSE for key atmospheric variables over a year forecast: (a) T850, (b) T2m, and (c) Z500. Results are shown for AtmosMJ with GRF (blue) and without GRF (red).

3.2 Quantitative evaluation against State-of-the-art models

Figure 3 compares the 10-day forecast RMSE of AtmosMJ against Pangu-Weather Bi et al. [2023], GraphCast Lam et al. [2022], and the IFS HRES operational forecast across six key meteorological variables. To ensure a fair comparison at the same spatial resolution (1.5°) as AtmosMJ, we report the deterministic scores of Pangu-Weather and GraphCast provided by WeatherBench 2. Despite being trained at higher resolutions, both models are evaluated after regridding to match the coarser scale. The results indicate that AtmosMJ achieves competitive long-range forecast accuracy, especially in upper-level variables such as Z500 and T850, maintaining lower error growth over time compared to deep learning counterparts.

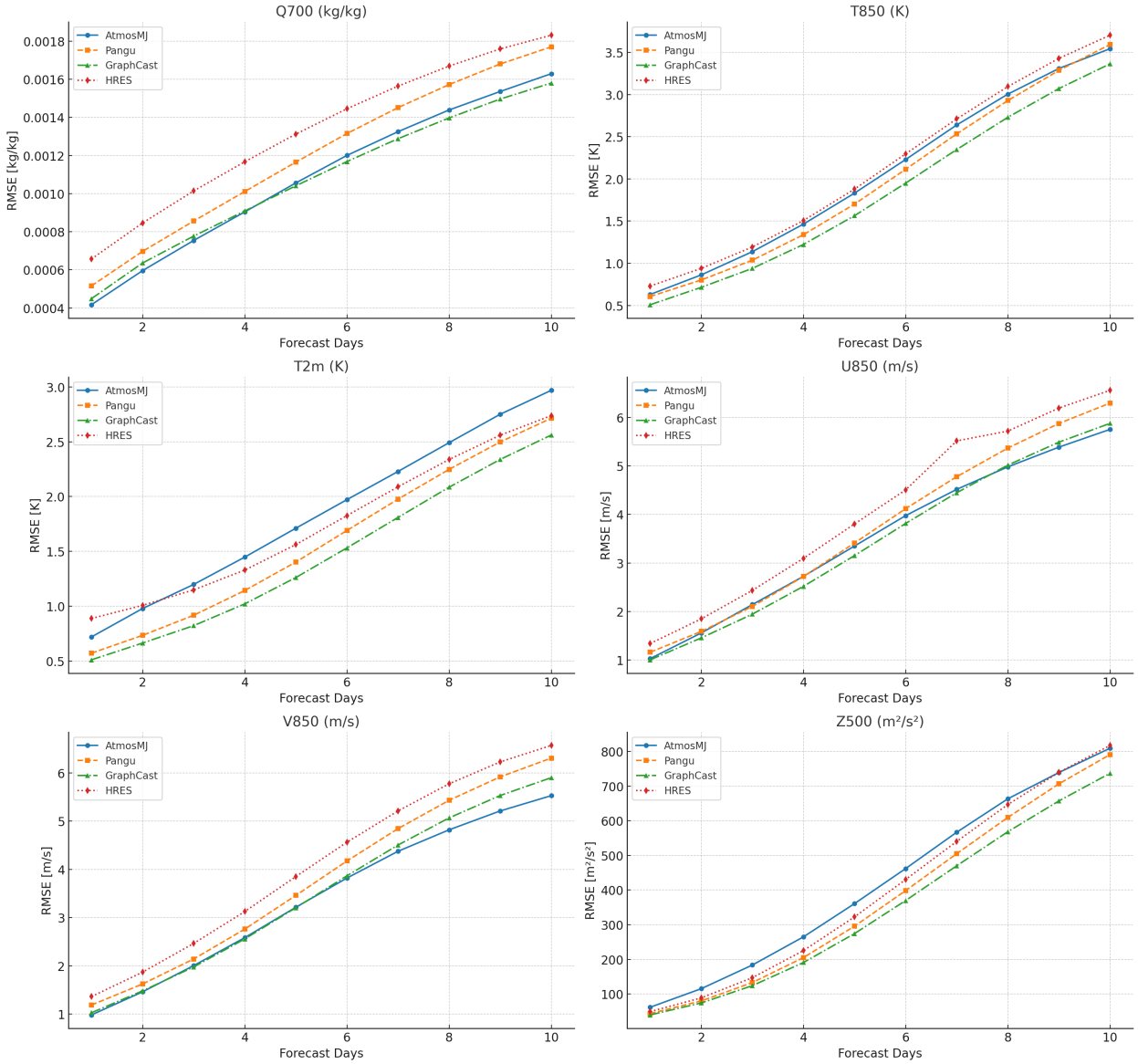

Figure 3: Global forecast performance of AtmosMJ versus state-of-the-art baselines. Latitude-weighted RMSE is shown for key variables over a 10-day horizon. Trained on lower-resolution data (1.5°), AtmosMJ matches Pangu-Weather and GraphCast, especially at longer lead times. For fairness, all baselines are evaluated at 1.5° using WeatherBench 2 deterministic scores.

Table 3 presents a quantitative comparison of recent AI-based global weather forecasting models using RMSE scores for selected variables at a 24-hour lead time. All evaluations are conducted using ERA5 data from the year 2020. The variables include geopotential at 500 hPa (Z500), temperature at 850 hPa (T850), specific humidity at 700 hPa (Q700), and wind components (U/V850), as well as near-surface temperature (T2m) Couairon et al. [2024a]. All models are either trained or evaluated at 1.5° resolution for a fair comparison.

Our model, AtmosMJ, achieves competitive performance across several key variables, showing similar or even better RMSE scores compared to more recent models such as Stormer and ArchesWeather-M. In particular, AtmosMJ records the lowest RMSE in Q700, U850, V850, and T2m. Notably, this is achieved with the smallest reported training cost—just 5.7 V100-days—highlighting AtmosMJ's high computational efficiency relative to the other models.

Table 3: Comparison of AI weather models on RMSE scores for key weather variables with 24-hour lead time at 1.5° resolution. All models are evaluated on 2020 ERA5 data. Results for Pangu-Weather, GraphCast, and HRES are taken from the ArchesWeather paper Couairon et al. [2024a]. Cost is the training computational budget in V100-days. Best scores for each variable are in bold.

Model	Res	Cost	Z500	T850	Q700	U850	V850	T2m
ArchesWeather-M Couairon et al. [2024a]	1.5°	11.0	48.10	0.65	0.00054	1.29	1.34	**0.55**
NeuralGCM ENS (50) Kochkov et al. [2023]	1.4°	7680.0	**43.99**	0.66	0.00054	1.24	1.26	**0.55**
Stormer Nguyen et al. [2023]	1.4°	256.0	45.12	**0.61**	0.00053	1.14	1.16	0.57
AtmosMJ	1.5°	**5.7**	62.94	0.63	**0.00045**	**1.03**	**0.99**	0.70

3.3 Long-Term Forecast Stability and Physical Plausibility

To evaluate large-scale atmospheric variability and seasonal evolution, we analyze the 3-day running mean of zonal-mean Z500 and T850 over a 500-day forecast initialized on January 2, 2018 (forecast days 1–499 correspond to January 3, 2018 through May 17, 2019). Applying a 3-day running mean suppresses short-term variability and clarifies long-term patterns. As shown in Figure 4, our proposed model successfully reproduces the meridional gradients and seasonal progression observed in the ERA5 reference, effectively capturing the coupled dynamics between mid-tropospheric temperature and geopotential.

In Z500, the model maintains the crucial latitudinal pressure contrast between mid- and high-latitudes. This reflects its strong ability to simulate the geopotential thickness variations driven by meridional temperature gradients, where warmer temperatures at lower latitudes lead to higher geopotentials, and vice versa. Although there is a slight underestimation of the amplitude poleward of 60° N/S, this aligns with a similar underestimation in T850, suggesting that the model effectively captures the physical coupling between temperature and geopotential even in these extreme regions.

For T850, the subtropical warm belt and the polar cold zone - along with their characteristic north-south migrations - are well captured throughout the year. This consistent representation of temperature patterns, coupled with the accurate Z500 fields, underscores the robust physical consistency of the model.

In contrast, the NVIDIA Earth2MIP implementation of GraphCast remains reasonable for only the first 1.5 months, and the DeepMind version degrades after just a couple of weeks. SFNO's Earth2MIP model (FourCastNetv2-small) and DLWP-HPX sustain realistic fields for about one year Karlbauer et al. [2024]. Our model, however, maintains realistic circulation and thermal contrasts for the full 500-day horizon, demonstrating its superior stability and physically consistent behavior over extended forecasts.

Figure 5 provides a stark comparison of model performance after 397 autoregressive steps, contrasting the versions of AtmosMJ with and without the Gated Residual Fusion (GRF) module against the ERA5 ground truth. The leftmost panel, representing the model without GRF, shows a complete simulation collapse into a physically unrealistic state, demonstrating catastrophic error accumulation. In stark contrast, the main AtmosMJ model with GRF (center panel) produces a stable and physically plausible forecast that aligns closely with the ERA5 ground truth (right panel). The model faithfully reproduces key large-scale circulation features, such as the polar vortex over the Arctic and zonally elongated troughs over East Asia and North America. The trough associated with the Aleutian Low, for instance, is realistically captured in both shape and location. This direct comparison highlights that the GRF mechanism is critical for ensuring long-term stability and preventing numerical divergence in extended forecasts.

Furthermore, the proposed model can generate a full 500-day forecast in approximately 21 seconds on a single GPU, highlighting its potential for practical and rapid long-range simulation.

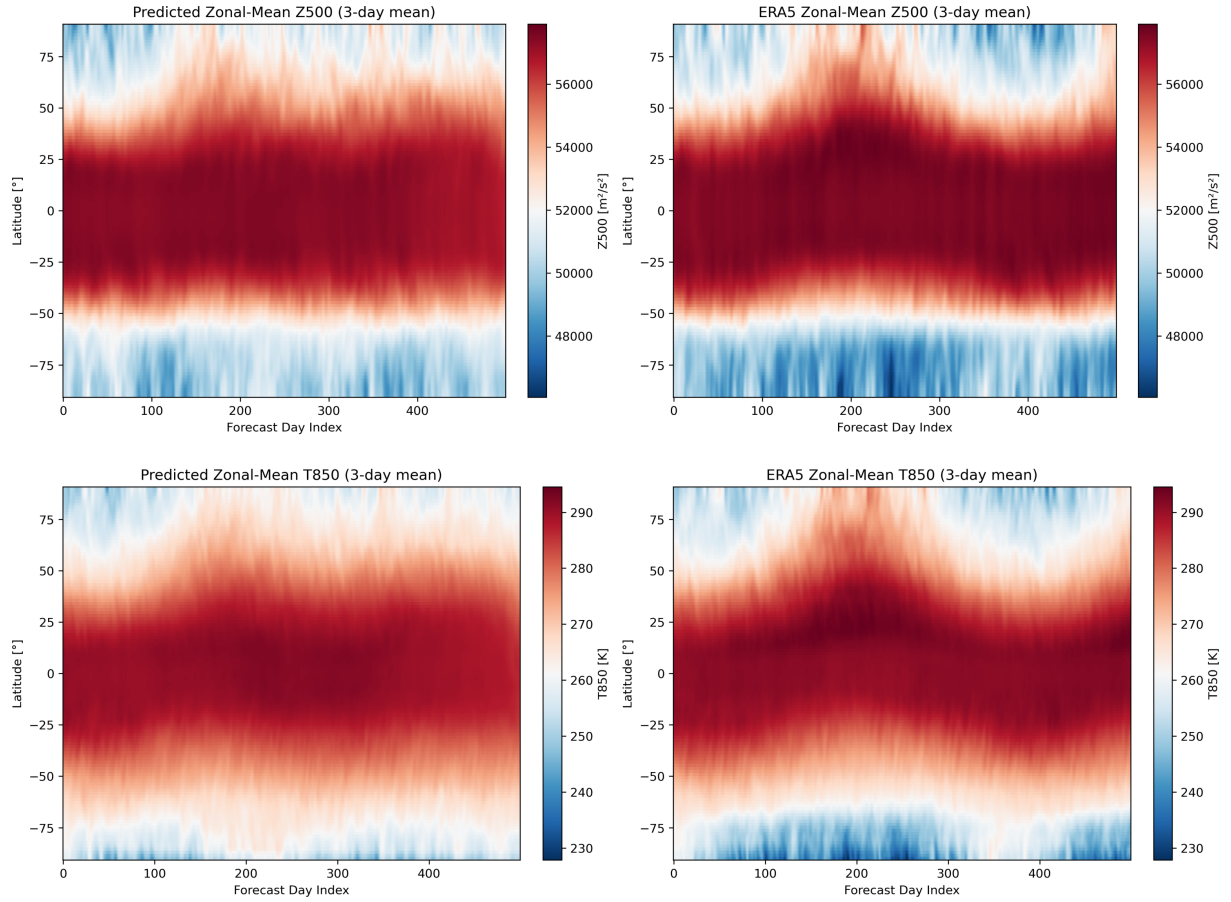

Figure 4: Comparison of 3-day-mean zonal-mean (top) Z500 and (bottom) T850 fields between the model predictions (left) and ERA5 reanalysis (right) over a 500-day rollout.

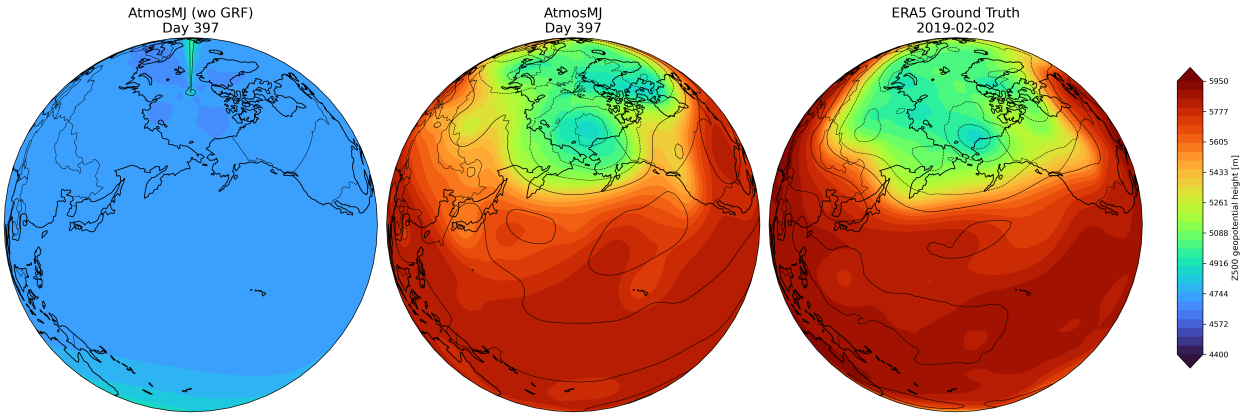

Figure 5: Comparison of 500 hPa geopotential height (Z500) and 1000 hPa height contours (Z1000) on simulation day 397 (2 February 2019). The figure compares forecasts from AtmosMJ without GRF (left) and with GRF (center) against the ERA5 ground truth (right).

As summarized in Table 4, our study highlights the feasibility of achieving long-term numerical stability directly on a conventional latitude–longitude grid. While prior models such as SFNO and DLWP-HPX relied on specialized coordinate systems (e.g., Spherical Harmonics and HEALPix) to produce stable forecasts beyond one year, AtmosMJ attains physically plausible forecasts for over 500 days without requiring any spatial transformation. This finding suggests that stability in long-range forecasting can be attributed more to the network architecture and computation scheme than to the complexity of the underlying spatial representation.

Table 4: Comparison of long-term forecasting models. AtmosMJ achieves year-scale stability without requiring specialized spatial transformations.

Model	**Grid Type**	**Stability**
SFNO Bonev et al. [2023]	Spherical Harmonics	1 year
DLWP-HPX Karlbauer et al. [2024]	HEALPix Mesh	1 year
AtmosMJ	Lat-Lon Grid	**500 days**

Acknowledgements

The author would like to express sincere gratitude to Jeong-Hwan Kim, Seon-Yu Kang, Yo-Hwan Choi, CoG, CoS, and Marco Lee for their valuable discussions and unwavering moral support throughout the course of this research. In particular, Jeong-Hwan Kim, Seon-Yu Kang, and Yo-Hwan Choi have been deeply supportive since the author's development of the author's first AI weather model, KARINA, and their continued encouragement has been truly invaluable. Special thanks to CoL for carefully reviewing the manuscript. This study was conducted independently with the generous financial support of the author's parents.

4 Conclusion

This study set out to answer a central question in the development of AI-based weather models: whether transforming atmospheric data onto non-standard spatial domains is a prerequisite for achieving long-term forecasting stability. Through the development and evaluation of our model, AtmosMJ, we have demonstrated that this is not the case. By operating directly on the conventional latitude-longitude grid, our model successfully generated stable, physically consistent forecasts for about 500 days, surpassing the year-long stability demonstrated by models reliant on specialized grids like spherical harmonics or HEALPix meshes.

Our primary contribution is the demonstration that architectural innovation can effectively replace the need for complex data transformations. The integration of the Gated Residual Fusion (GRF) mechanism proved critical in mitigating the long-term error accumulation that typically plagues autoregressive models, enabling a stable rollout far beyond the medium range. Qualitatively, AtmosMJ accurately captured key features of global circulation, including seasonal cycles and large-scale pressure systems, for the entire 500-day simulation. Quantitatively, it delivered competitive short-range forecast accuracy compared to existing models such as Pangu-Weather, GraphCast, and Stormer.

Remarkably, these results were achieved with exceptional computational efficiency, requiring only 5.7 V100-days for training. This significantly reduces the entry barrier for developing consistent long-range weather models. In conclusion, our work successfully decouples architectural design from data representation in the pursuit of long-term stability, highlighting a promising and more direct path toward building the next generation of efficient and accessible Large Weather Models.

References

Jay Chempan and contributors. Awesome lwms: A curated list of lightweight weather models. `https://github.com/jaychempan/Awesome-LWMs`, 2024. Accessed: 2025-06-08.

Kaifeng Bi, Lingxi Xie, Hengheng Zhang, Xin Chen, Xiaotao Gu, and Qi Tian. Accurate medium-range global weather forecasting with 3d neural networks. *Nature*, 619(7970):533–538, 2023.

Remi Lam, Alvaro Sanchez-Gonzalez, Matthew Willson, Peter Wirnsberger, Meire Fortunato, Ferran Alet, Suman Ravuri, Timo Ewalds, Zach Eaton-Rosen, Weihua Hu, et al. Graphcast: Learning skillful medium-range global weather forecasting. *arXiv preprint arXiv:2212.12794*, 2022.

Dmitrii Kochkov, Janni Yuval, Ian Langmore, Peter Norgaard, Jamie Smith, Griffin Mooers, Milan Klöwer, James Lottes, Stephan Rasp, Peter Düben, Sam Hatfield, Peter Battaglia, Alvaro Sanchez-Gonzalez, Matthew Willson, Michael P. Brenner, and Stephan Hoyer. Neural General Circulation Models for weather and climate. *arXiv preprint arXiv:2311.07222*, 2023.

Jaideep Pathak, Shashank Subramanian, Peter Harrington, Sanjeev Raja, Ashesh Chattopadhyay, Morteza Mardani, Thorsten Kurth, David Hall, Zongyi Li, Kamyar Azizzadenesheli, et al. Fourcastnet: A global data-driven high-resolution weather model using adaptive fourier neural operators. *arXiv preprint arXiv:2202.11214*, 2022.

Lei Chen, Xiaohui Zhong, Feng Zhang, Yuan Cheng, Yinghui Xu, Yuan Qi, and Hao Li. Fuxi: A cascade machine learning forecasting system for 15-day global weather forecast. *arXiv preprint arXiv:2306.12873*, 2023.

Tung Nguyen, Rohan Shah, Hritik Bansal, Troy Arcomano, Romit Maulik, Veerabhadra Kotamarthi, Ian Foster, Sandeep Madireddy, and Aditya Grover. Stormer: Scaling transformer neural networks for skillful and reliable medium-range weather forecasting. *arXiv preprint arXiv:2312.03876*, 2023.

Guillaume Couairon, Christian Lessig, Anastase A. Charantonis, and Claire Monteleoni. ArchesWeather: An efficient ai weather forecasting model at 1.5° resolution. *arXiv preprint arXiv:2405.14527*, 2024a.

Lei Chen, Xiaohui Zhong, Hao Li, Jie Wu, Bo Lu, Deliang Chen, Shang-Ping Xie, Libo Wu, Qingchen Chao, Chensen Lin, et al. A machine learning model that outperforms conventional global subseasonal forecast models. *Nature Communications*, 15(1):6425, 2024.

Boris Bonev, Thorsten Kurth, Christian Hundt, Jaideep Pathak, Maximilian Baust, Karthik Kashinath, and Anima Anandkumar. Spherical fourier neural operators: Learning stable dynamics on the sphere. *arXiv preprint arXiv:2306.03838*, 2023.

Matthias Karlbauer, Nathaniel Cresswell-Clay, Dale R. Durran, Raul A. Moreno, Thorsten Kurth, Boris Bonev, Noah Brenowitz, and Martin V. Butz. Advancing parsimonious deep learning weather prediction using the HEALPix mesh. *Journal of Advances in Modeling Earth Systems*, 16(8):e2023MS004021, 2024. doi:10.1029/2023MS004021.

Guillaume Couairon, Christian Lessig, Anastase Charantonis, and Claire Monteleoni. Archesweather: An efficient ai weather forecasting model at 1.5 {\deg} resolution. *arXiv preprint arXiv:2405.14527*, 2024b.

Stephan Rasp, Stephan Hoyer, Alexander Merose, Ian Langmore, Peter Battaglia, Tyler Russell, Alvaro Sanchez-Gonzalez, Vivian Yang, Rob Carver, Shreya Agrawal, et al. Weatherbench 2: A benchmark for the next generation of data-driven global weather models. *Journal of Advances in Modeling Earth Systems*, 16(6):e2023MS004019, 2024.

Weihao Yu, Pan Zhou, Shuicheng Yan, and Xinchao Wang. Inceptionnext: When inception meets convnext. In *Proceedings of the IEEE/cvf conference on computer vision and pattern recognition*, pages 5672–5683, 2024.

Minjong Cheon, Yo-Hwan Choi, Seon-Yu Kang, Yumi Choi, Jeong-Gil Lee, and Daehyun Kang. Karina: An efficient deep learning model for global weather forecast. *arXiv preprint arXiv:2403.10555*, 2024.

Junyoung Chung, Caglar Gulcehre, KyungHyun Cho, and Yoshua Bengio. Empirical evaluation of gated recurrent neural networks on sequence modeling. arxiv 2014. *arXiv preprint arXiv:1412.3555*, 1412, 2014.